

See discussions, stats, and author profiles for this publication at: <https://www.researchgate.net/publication/257620523>

The Effect of Surface Properties in Activated Carbon on Mercury Adsorption

ARTICLE *in* INDUSTRIAL & ENGINEERING CHEMISTRY RESEARCH · JUNE 2012

Impact Factor: 2.59 · DOI: 10.1021/ie2028156

CITATIONS

5

READS

77

6 AUTHORS, INCLUDING:



Xiaolong Yao

Tsinghua University

19 PUBLICATIONS 38 CITATIONS

[SEE PROFILE](#)



Xin Li

University of Cincinnati

12 PUBLICATIONS 48 CITATIONS

[SEE PROFILE](#)



Joo-Youp Lee

University of Cincinnati

66 PUBLICATIONS 365 CITATIONS

[SEE PROFILE](#)



Tim C. Keener

University of Cincinnati

190 PUBLICATIONS 1,156 CITATIONS

[SEE PROFILE](#)

The Effect of Surface Properties in Activated Carbon on Mercury Adsorption

Liqing Li,^{†,*} Xin Li,[‡] Joo-Youp Lee,[‡] Tim C. Keener,[‡] Zheng Liu,[†] and Xiaolong Yao[†]

[†]School of Energy Science and Engineering, Central South University, Changsha 410083, Hunan, China.

[‡]Department of Civil and Environmental Engineering, University of Cincinnati, Cincinnati, Ohio 45221, United States

ABSTRACT: Physical and chemical properties of raw and modified activated carbon were analyzed to investigate the effects of adsorbate properties on activated carbon adsorption performance. Mercury adsorption was tested by cupric chloride impregnated activated carbon, which used water, acetone, and isopropyl alcohol as solutions. The results indicated that the adsorption capacity of Hg⁰ in the cupric chloride impregnated activated carbon in isopropyl alcohol was the greatest. Accumulation of Cu on the modified activated carbon surface and other oxygen functional groups was key in affecting the chemisorption of mercury. Two degradation steps were observed in TGA-MS measurements. Decomposition of functional groups containing two oxygen atoms in modified activated carbon took place in the first step, whereas most residual organic groups in activated carbon were primarily decomposed in a second step from 300 to 400 °C, the more organic groups present, the lower the temperature of thermal degradation.

1. INTRODUCTION

Coal-fired utility boilers are the largest source of anthropogenic mercury, accounting for 33% of the total mercury emissions.¹ The emission of mercury from coal combustion is primarily in the elemental form Hg⁰ which has been recognized to demonstrate both acute and chronic toxicity with respect to the nervous, renal, and reproductive systems.² Recently, mercury emissions from coal-combustion flue gases have become a major environmental concern, and have presented the need for efficient mercury control technology. Activated carbon (AC) is well-established as a good adsorbent of various kinds of airborne contaminants.³ Most of the reported adsorption studies have been carried out at or around room temperature, whereas the temperature of flue gas would be above 400 K. Due to mercury's high volatility and weak bonding onto carbon surfaces, it is likely that virgin activated carbon alone is an ineffective adsorbent for most practical applications.

One method for overcoming this deficiency is to impregnate the surface of activated carbon with reagents such as sulfur, halides, thiols, and active functional groups. Sulfur^{4,5} and iodine^{6,7} are typical impregnates for respirator cartridge applications. Work by Vidic⁸ demonstrated that thiol-impregnated activated carbon performed well at adsorbing mercury vapor at room temperature. Lee^{9,10} investigated the Hg oxidation and adsorption mechanisms of mercury with cupric chloride-impregnated AC in fixed-bed, entrained-flow, and filter-added entrained-flow systems. Padak¹¹ reported a theoretical interpretation for the enhanced mercury-bonding properties of halide- and oxide-impregnated carbon surfaces based on a density functional theory. Y. H. Li¹² studied the importance of activated carbon's oxygen surface functional groups on elemental mercury adsorption by means of heat and acid treatment.

The adsorption at low temperatures may only be dependent on the adsorbate–adsorbent interactions between the solid and the adsorbate molecule. Adsorption at high temperatures will rely not only on physical intermolecular forces, but will more

importantly rely on the chemical bond strength between molecules. All of the above sources have shown that AC and its associated physical surface and chemical properties are the most important factors influencing Hg⁰ adsorption. The decisive role of surface chemistry on the adsorption properties of carbon materials has long been recognized,^{13,14} but only recently has it become possible to derive useful quantitative relationships.¹⁵

Different activated carbons have been examined in bench-, pilot-, and full-scale tests; however, correlations between the physical and chemical characteristics of AC and its Hg⁰ adsorption properties have not been established. The mechanisms involved in Hg⁰ adsorption are not well understood. Adsorption of mercury by AC is complex and may involve physical adsorption, chemical reaction, electrostatic effects and coordination with functional groups on AC surfaces. Several factors, such as specific surface area, pore-size distribution, pore volume, surface charge, and presence of surface functional groups, affect the adsorption of mercury on to AC. In the present study, we have investigated the influence of active surface groups on the adsorption of Hg⁰ from simulated flue gas on modified AC. Furthermore, we have attempted to ascertain the real nature of the adsorbed cupric chloride impregnated carbon surface interactions using Fourier transform infrared spectroscopy (FTIR), thermogravimetric analysis (TGA) and temperature programmed desorption (TPD) measurements.

2. EXPERIMENT MATERIALS AND METHODS

2.1. Materials. Commercial activated carbon manufactured by Norit Americas Inc. (Marshall, TX) and cupric chloride impregnated activated carbon synthesized in our laboratory were used in this study.

Received: December 2, 2011

Revised: May 30, 2012

Accepted: June 13, 2012

Published: June 13, 2012

A specific quantity of cupric chloride hydrate ($\geq 99.0\%$ $\text{CuCl}_2 \cdot 2\text{H}_2\text{O}$; Aldrich Chemical Co., Milwaukee, WI) was dissolved in 100 mL isopropyl alcohol (IPA) (99.8%; Pharmco Products Inc., Brookfield, CT), acetone (99.8%; Pharmco Products Inc., Brookfield, CT) and distilled water. To the mixture, 10 g commercial, raw activated carbon (DARCO Hg; Norit Americas Inc., Marshall, TX) was added slowly, and the mixture remained at room temperature for approximately 3 h with continuous stirring. The solution was filtered and the resulting solid was dried at 100 °C for approximately 2 h to create three types of modified AC, cupric chloride impregnated activated carbon in IPA ($\text{CuCl}_2\text{-AC-IPA}$), cupric chloride impregnated activated carbon in acetone ($\text{CuCl}_2\text{-AC-acetone}$), cupric chloride impregnated activated carbon ($\text{CuCl}_2\text{-AC-water}$), respectively. Cupric chloride dissolved well in water; the solubility of cupric chloride in isopropyl alcohol and water at room temperature (23 °C) is 23.7% and 43.8%, respectively, and is blue in color.¹⁶ Cupric chloride is difficult to dissolve in acetone solutions and a dark red precipitate forms after stirring for 2 h. The filtered solution also appears dark red in color. The species $[\text{Cu}(\text{H}_2\text{O})_6]^{2+}$ and $[\text{Cu}((\text{CH}_3)_2 = \text{CH}-\text{OH})_x]^{2+}$ are blue in water and isopropyl alcohol solutions. The third species is red and is a halide complex of the formula $[\text{CuCl}_{2+x}]^{x-}$ in acetone due to its insolubility.¹⁷ The following conclusion can be drawn: copper in isopropyl alcohol and water were adsorbed in the form of cupric ions onto activated carbon by means of ion exchange, while copper in acetone was impregnated in the form of cupric chloride complex salt molecules onto activated carbon. All filtered solutions were analyzed for residual concentrations of copper and chloride in the solution using an atomic absorption spectrophotometer (Analyst 300, Perkin-Elmer, Waltham, MA) for copper and ion chromatography (DX-600, Dionex, Sunnyvale, CA) for chloride.

2.2. Fixed-Bed System and Experimental Procedure.

A fixed-bed adsorption system was constructed as shown in Figure 1.

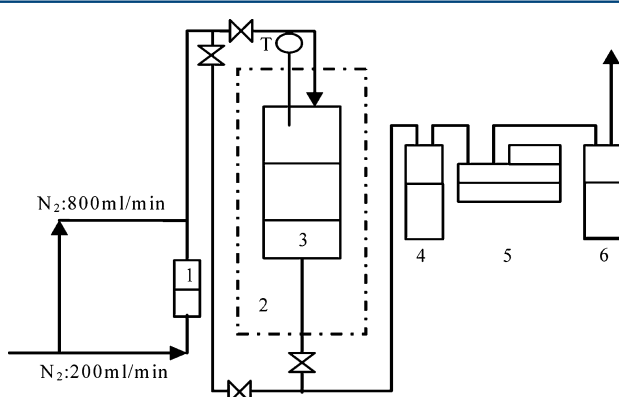


Figure 1. Schematic of a fixed-bed system 1: Mercury permeation tube; 2: Oven; 3: Adsorption fixed-bed; 4: Scrubbing tube for ionic mercury with 1 M KCl; 5: Mercury analyzer; 6: Scrubbing tube for total mercury.

The 1.27 cm diameter adsorption column made of borosilicate glass was placed inside a temperature-controlled convection oven (Stabil-Therm Electric Utility Oven, Model OV-500C-2, Blue M Electric Company, New Columbia, PA) at a temperature of 140 °C. A sorbent sample was mixed in silica (SiO_2 , Fisher Scientific, fine granules, particle size: 149–420 nm) prior to being packed in the adsorption column. Approximately 20 mg of

each sorbent was premixed with 4 g of silica (fine granules, 40–100 mesh, Fisher Scientific Inc, Pittsburgh, PA) and placed in the fixed bed. A total air flow rate of 1 $\text{L}\cdot\text{min}^{-1}$ was provided to the fixed bed. An Hg^0 -laden gas stream was generated from elemental mercury permeation tubes (VICI Metronics, Inc., Poulsbo, WA), and the flow rate was maintained at 200 $\text{mL}\cdot\text{min}^{-1}$ using a mass flow controller. An additional air flow of 800 $\text{mL}\cdot\text{min}^{-1}$ was injected into the fixed bed. The total flow rate was also monitored using a bubble flow meter. The outlet mercury speciation was conducted by using the Ontario Hydro Method.¹⁸ A 1 M KCl solution was used to capture oxidized mercury. The outlet Hg^0 concentration was also observed by an inline mercury analyzer (UV-1201S with mercury analysis kit, Shimadzu Corp., Columbia, MD), and an acidified KMnO_4 solution was used to capture elemental mercury from the effluent gas. After each test, the spent sorbent was collected and analyzed for the amount of mercury adsorbed by following the digestion procedures described in the Ontario Hydro Method.

2.3. Experimental Methods. The specific surface area and pore diameter of the AC were measured using a specific apparatus¹⁹ (SA3100, Beckman Company). The adsorption isotherm of nitrogen was measured at 77.131 K using the volumetric method. The specific surface area was calculated using the BET method. The microporous specific surface area of pores smaller than 2 nm, mesopore volume of pores between 2 and 50 nm,²⁰ the external surface area, as well as its volumes were calculated using the t-Plot method. The pore diameter distribution was measured using the BJH method, which analyzes the branches of the adsorption and desorption isotherms. The surface texture of the AC was captured with a scanning electron microscope (SEM; S-3000N SEM, Hitachi Ltd., Japan).

The chemical properties of the AC surface were estimated by standard neutralization titration with HCl , NaHCO_3 , Na_2CO_3 and NaOH (0.1 M) according to Boehm's method.²¹

Boehm titration was applied to quantitatively determine the acidic and basic surface functional groups/sites on the prepared AC.²⁵ Eight hundred milligrams of the prepared AC and either 25 mL of NaHCO_3 (0.1 mol·L⁻¹), Na_2CO_3 (0.1 mol·L⁻¹), or NaOH (0.1 mol·L⁻¹) was mixed in a conical flask, agitated at 100 rpm for 4 days at 298 K, and a 10 mL aliquot of each sample solution was back-titrated with HCl (0.1 mol·L⁻¹). The NaHCO_3 neutralizes only carboxylic groups on the carbon surface, Na_2CO_3 neutralizes carboxylic and lactonic groups, and NaOH reacts with carboxylic, lactonic and hydroxyl groups. Accordingly, the difference between the groups neutralized by NaHCO_3 and Na_2CO_3 is the lactones, and the difference between those neutralized by Na_2CO_3 and NaOH is the hydroxyls. The same procedure was carried out for a mixture of 0.8 g of the carbons and 25 mL of HCl (0.1 mol·L⁻¹) solution to determine the basic sites on the carbon surface. After an excess amount of NaOH (0.1 mol·L⁻¹) solution was added to the remaining HCl solution, the NaOH solution was titrated with HCl (0.1 mol·L⁻¹) solution again. Neutralization points were detected using methyl red solution indicator for a weak base titrated with strong acid, and phenolphthalein solution for a strong acid and strong base combination.

Surface chemistry of the AC was studied by FTIR, TPD, and TGA-MS. The FTIR spectra were recorded by computer interfaced Shimadzu 8400S FTIR spectrometer between 750 and 4600 cm^{-1} . TPD experiments were carried out by heating the samples to 1273 K under He gas flow at a heating rate of 10 K/min, and the amounts of desorption materials were recorded with a Balzers Thermocube quadrupole mass

Table 1. Specific Surface Areas and Pore Volumes of AC

sample	S_{BET} $\text{m}^2 \cdot \text{g}^{-1}$	S_{mic} $\text{m}^2 \cdot \text{g}^{-1}$	S_{ext} $\text{m}^2 \cdot \text{g}^{-1}$	ν_{total} $\text{cm}^3 \cdot \text{g}^{-1}$	ν_{mic} $\text{cm}^3 \cdot \text{g}^{-1}$	total microporosity ratio
AC	471.815	199.393	272.422	0.494	0.106	4.67

spectrometer as a function of temperature, as described elsewhere.²² The thermal decomposition pathways of mercury-adsorbed carbon were examined using TGA (Q5000IR, TA Instruments) inline coupled with a quadrupole mass spectrometer (MS, Pfeiffer Vacuum Ltd.), with flexible heated silica lined steel capillary tubing and a molecular leak.

3. RESULTS AND DISCUSSION

3.1. Physical properties of AC. The specific surface areas and pore volumes are shown in Table 1. Specifically, Table 1 presents the BET surface area (S_{BET}), microporous specific surface area (S_{mic}), external surface area (S_{ext}), total pore volume (ν_{total}), and the micropore volume (ν_{mic}) for each AC used in the study. The ratio of total pore volume to micropore volumes was employed to evaluate the structural parameters along with the degree of porosity. The total microporosity ratio²³ was 4.67, demonstrating that the AC exhibited micropores in its structure with a relatively smaller microporous volume of $0.106 \text{ cm}^3 \cdot \text{g}^{-1}$. Therefore, the mesopores and macropores volume was $0.388 \text{ cm}^3 \cdot \text{g}^{-1}$.

To explain the surface characteristics of AC, the porosity and surface chemistry should be taken into consideration. Figure 2

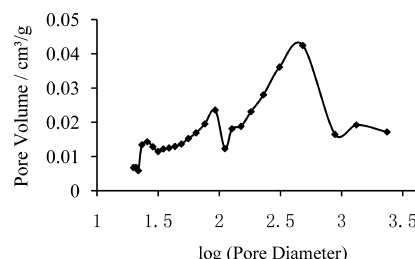


Figure 2. Pore size distributions of AC used in the study.

shows pore size distributions of the carbon materials and pore volumes at different pore sizes. A log scale of pore diameter size for the x -axis was used. As shown in this figure, the pore diameter distribution ranged extensively from 19 to 2500 nm and had a multimodal distribution; peaks occurred when the diameter was 25.76 nm, 92.52 nm, and 481.36 nm, and its macropores were the most numerous with a proportion of 62%.

3.2. Chemical Properties of AC. Figure 3 displays SEM images of the AC and shows some spots of various dimensions and intensities that irregularly cover the particle surface. In Figure 3, one characteristic zone has been selected. The results of EDS microanalysis carried out on the selected zone are also reported in Table 2. This table shows that in the selected zone, high oxygen and sulfur concentrations are present.

The amount of oxygen corresponds to approximately 8.41% of the total numbers of elements for raw AC. Some of the elements exist as metal oxides and others are carbon oxygen compounds that constitute surface organic functional groups of activated carbon. The performance of adsorption, specifically chemical adsorption, depends on such suitable active sites that are capable of chemisorbing the reactants and forming surface intermediates of adequate strength.²⁴

The surface characteristics of the activated carbons are tabulated in Table 3. It was found that when increasing the

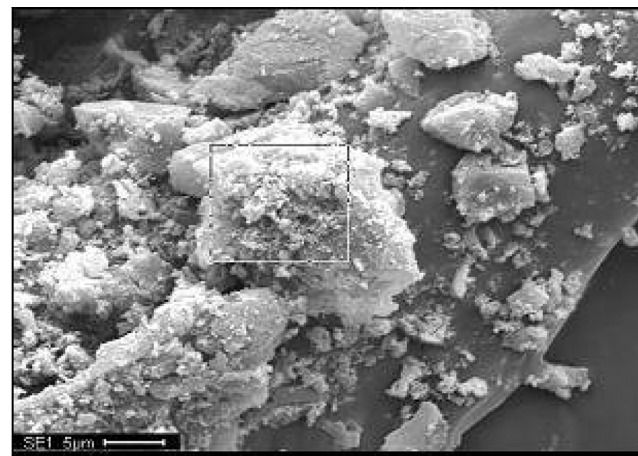


Figure 3. SEM micrograph of raw carbon.

amount of cupric chloride deposition in the same solution, little change could be seen in the number of active groups on the AC.

The titration results presented in Table 3 suggest that all the carbonaceous sorbents possess oxygen functionalities in the form of noncarbonyl (i.e., carboxylic, lactonic and hydroxyl groups) and carbonyl²⁶ surface functional groups. Figueiredo²⁴ summarized the different oxygen functional groups that can be found on carbon surfaces in Figure 4.

The concentration of strongly acidic groups increases greatly after treatment with cupric chloride impregnated AC. Carboxylic groups are considered to be strongly acidic, in comparison with other oxygen containing groups on the carbon surface, such as the phenolic, lactonic, and quinone groups. The carboxylic groups have the lowest pK values, and phenolic groups possess the highest pK values.²⁷ The number of carboxylic groups increased by 28.6% (CuCl_2 -AC-water), 46.7% (CuCl_2 -AC-acetone) and 54.9% (CuCl_2 -AC-IPA) after modification with cupric chloride. Multiple increases in hydroxyl groups with the introduction of cupric chloride are also observed, as shown in Table 3. Compared to the carboxylic groups and hydroxyl groups, lactone groups increased slightly after cupric chloride immersion in isopropyl alcohol and in acetone solutions. Lactones decreased with cupric chloride soaked in water, but their fluctuations were not large. Treatment with acetone and IPA together with cupric chloride can obviously increase the acidic sites on the AC such as phenols, carboxyls or carbonyls, as compared with the original activated carbon. The treatment can slightly decrease the acidic sites on the AC, such as lactones and lactols after treatment with cupric chloride in water.²⁶ The surface nature was changed by the oxidation when the cupric chloride acted as a catalyst in IPA and acetone solutions, introducing carboxylic, lactonic, and phenolic groups onto the AC. This result occurred because of the introduction of Cu^{2+} (Lewis acids²⁸) on the carbon surface with oxygen-containing groups by ion exchange, enhancing the acetone and IPA chemisorption and changing them to acidic groups. The chemisorbed capacity per cation is proportional to the electronegativity (Lewis acidity) of the metal ions.

3.3. Mercury Adsorption. In order to estimate the influence of AC's surface characteristics, Hg^0 adsorption studies

Table 2. Local Composition (%) Obtained by EDS Microanalysis of Raw Carbon Samples

elements	C	O	Mg	Al	Si	S	Cl	Ca
composition /%	85.93	08.41	00.62	00.56	02.16	00.41	00.00	01.91

Table 3. Chemical Surface Groups of AC

items (mmol·g ⁻¹)	total basic	total acidic	hydroxyl	lactones	carboxyl
raw AC	1.760	1.262	0.032	0.829	0.402
6.5%CuCl ₂ -AC-IPA	1.981	1.795	0.191	0.982	0.622
6.5%CuCl ₂ -AC-acetone	1.850	1.588	0.157	0.842	0.589
6.5%CuCl ₂ -AC-water	1.595	1.133	0.077	0.539	0.517

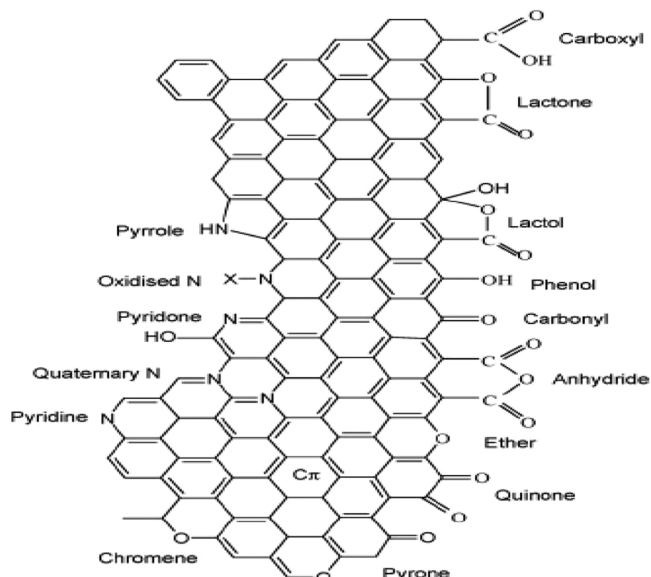
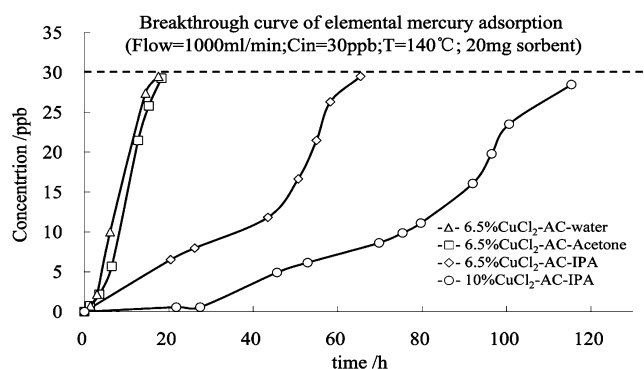


Figure 4. Nitrogen and oxygen surface groups on carbon.

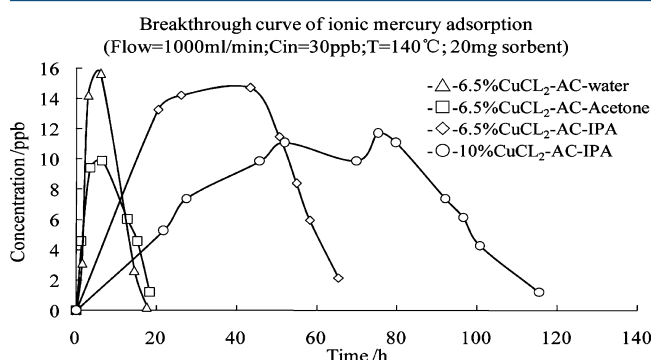
on CuCl₂-AC-IPA, CuCl₂-AC-acetone and CuCl₂-AC-water, were conducted on the fixed bed reactor under an N₂ environment. The adsorption process was only influenced by AC's surface characteristics. The result could reflect the impact of AC's surface characteristics on Hg⁰ adsorption.

Figure 5 shows the Hg⁰ adsorption by cupric chloride impregnated AC under an N₂ environment. At this process of

Figure 5. Hg⁰ adsorption on cupric chloride impregnated AC under a N₂ environment.

experiment, the inlet Hg⁰ concentration was 30 ppb. The breakthrough curves of Hg⁰ were influenced by different solutions of cupric chloride. In the adsorbing phase, the larger the slope of the break through curve, the more rapidly the AC

to reach saturation, the shorter the mass transfer area it has, and the earlier it reaches adsorption balance. According to Figure 5, From the graph, the concentration of the Hg⁰, which the CuCl₂-AC-acetone and CuCl₂-AC-water increased rapidly to reach 30 ppb, and that the CuCl₂-AC-IPA increased more slowly. It is observed that the CuCl₂-AC-IPA has the greatest adsorption of elemental mercury, followed by the CuCl₂-AC-acetone, and the lowest is CuCl₂-AC-water. Because of the special additional cupric chloride and surface functional acidic groups deposited, the mercury adsorbed by the CuCl₂-AC-IPA at breakthrough was significantly higher than the mercury adsorption capacity of the impregnated carbon in other solutions at equilibrium. The values were higher than the mercury adsorbed at breakthrough in the blank run. From the outflow gas, ionic mercury was detected, which is presented in Figure 6.

Figure 6. Hg²⁺ outflow from cupric chloride impregnated AC under a N₂ environment.

Compared to Figure 5, it is clear that the amount of mercury ions increases in outflow gas of the adsorption with an increasing load of mercury on AC. Because ionic mercury existed in the outflow gas, it can be stated that adsorption by cupric chloride impregnated AC was mainly effected by chemical adsorption. Therefore, copper and surface groups on activated carbon, and their state of existence, will become a key factor in the chemisorption of mercury.²⁹

By increasing the uptake of cupric chloride on AC in IPA solution, the breakthrough curves of mercury adsorption can be moved horizontally from left to right. During the adsorption process, along with the increased adsorption time, the outlet Hg⁰ concentration increased gradually and the higher concentration of cupric chloride is, the more gentle was the trend of Hg⁰ adsorption to a final concentration to 30 ppb. Compared to the Hg⁰ trend, at the beginning, the outflow concentration of Hg²⁺ increased, and then decreased when it reached the highest value. Similar to Hg⁰, a more gentle change in Hg²⁺ concentration in 10% cupric chloride solution occurred. The deposited cupric chloride appeared to improve the mercury adsorption capacity of the cupric chloride-impregnated activated carbon because of the increased number of available equivalent chemical reactions.

Adsorption results are summarized in Table 4.

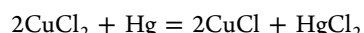
In Table 4, the Chemisorption data for the four different cupric chloride impregnated modified AC were calculated for varying amounts of cupric chloride and solutions. One obvious

Table 4. Mercury Chemisorption of AC

items	uptake of Hg ⁰ mg·(gAC) ⁻¹	Hg ²⁺ of outflow mg·(gAC) ⁻¹	total adsorbed Hg mg·(gAC) ⁻¹	adsorbed Cu/ uptake of Hg ⁰ mol·mol ⁻¹
6.5%CuCl ₂ -AC-IPA	31.908	19.350	12.559	3.026
10%CuCl ₂ -AC-IPA	44.350	33.601	10.749	2.178
6.5%CuCl ₂ -AC-acetone	7.816	2.783	5.032	12.358
6.5%CuCl ₂ -AC-water	6.928	3.935	2.993	17.159

trend was an increase in uptake of Hg⁰ and outflow of Hg²⁺ as the total amount of adsorbed Cu was increased. The effect of the bathing solution on mercury adsorption is also shown in Table 4. Three different solutions were used for modification, and the sample with the highest mercury uptake was the AC in IPA solution, although they all had the same copper content (6.5 wt.%). It can be stated that the copper content does not have a direct influence on the mercury uptake, but the distribution status of copper and its corresponding functional groups plays an important role in mercury adsorption on AC.

In addition, the results in Table 4 show that Hg⁰ oxidation of cupric chloride impregnated modified AC is almost completed after the adsorption equilibrium. Based on the Hg⁰ oxidation capacity of cupric chloride impregnated modified AC determined from the fixed-bed tests, the total amount of cupric chloride in sorbent used for Hg⁰ oxidation is determined as the molar ratio. The ratio of adsorbed Cu to the uptake of Hg⁰ is nearly 2:1 on the CuCl₂-AC-IPA. Therefore, the chemical adsorption mechanism can be accurately predicted as the following:



Copper ions, which exist as forms of $[\text{Cu}((\text{CH}_3)_2 = \text{CH}-\text{OH})\text{X}]^{2+}$, were evenly distributed on the active sites in the modified AC in IPA solution. These polar acidic groups have a stronger attraction to the electronic cloud of copper ions, making the copper(II) more accessible to the electrons of mercury, and easily reduced to cuprous. Copper ions on AC that was cupric chloride impregnated in water have a relatively weak reduction performance because of water having weak polarity and fewer active groups on the AC. Because cupric chloride is slightly soluble in acetone, cupric chloride adsorbed on AC will form agglomerated flocs. The reaction between copper(II) and Hg⁰ will be hindered because the reaction product covers its surface.

3.4. Fourier Transform Infrared (FTIR) Spectroscopy Analysis.

In order to obtain information concerning the changes in the surface groups associated with variations in the acidic/basic character of the samples, and for the reaction products related to chemical adsorption, FTIR characterization was carried out. It is observed from Figure 7 that several absorption peaks appear in the four FTIR spectra of the raw carbon and different cupric chloride impregnated AC with different intensities.

FTIR transmission spectra of adsorbed sorbents are shown in Figure 8. The spectra of the adsorbed AC bands of 3200–3640 cm⁻¹ and 2300–2500 cm⁻¹ were much weaker than that of the original carbons, demonstrating that the hydroxyl groups and carboxyl groups have changed in the process of chemisorption. Compared to the spectrum of the adsorbed AC-water, more pronounced bands at 3050–3600, 2800–3000, 1000–1120, and 880 cm⁻¹ were presented by adsorbed AC-IPA and adsorbed AC-acetone, which was similar to those of pure cupric chloride. This result indicated that cupric chloride was still present on these adsorbed AC. In contrast to the spectrum, the unique vibration bands at 863 and 808 cm⁻¹ of pure cuprous chloride can be seen on spectra of adsorbed AC, suggesting that cuprous chloride may occur on the adsorbed carbon.

Comparison of the FTIR spectrum of the AC-IPA sample with that of other materials shows that strong bands are observed at 3200–3640 cm⁻¹; these bands are assigned to the O–H stretching vibration due to the existence of surface hydroxyl groups.³⁰ The bands at 2300–2500 cm⁻¹ and 1600–1735 cm⁻¹ observed for all samples are the characteristic of O–H stretch for carboxylic acids.³¹ These sorbents have relatively stronger bands after cupric chloride impregnation, demonstrating that carboxyl groups are produced in these samples upon modification. Samples show a band at 1740 cm⁻¹ that can be assigned to lactone groups.³² Peaks are detected around 1400 cm⁻¹ for AC, which are attributed to the C–O stretching mode in the ester group. The peak at 1200–1300 cm⁻¹ is assigned to the C–C–O stretching mode³³ in unsaturated hydroxyl groups, which is obviously present on AC-IPA when compared to other AC. Bands below 850 cm⁻¹ are characteristic of out-of-plane deformation vibrations of C–H groups in aromatic structures, and this phenomenon, with higher intensities of the band, is clearly evident in the AC-IPA. When the spectrum of AC-IPA is compared to that of other sorbents,

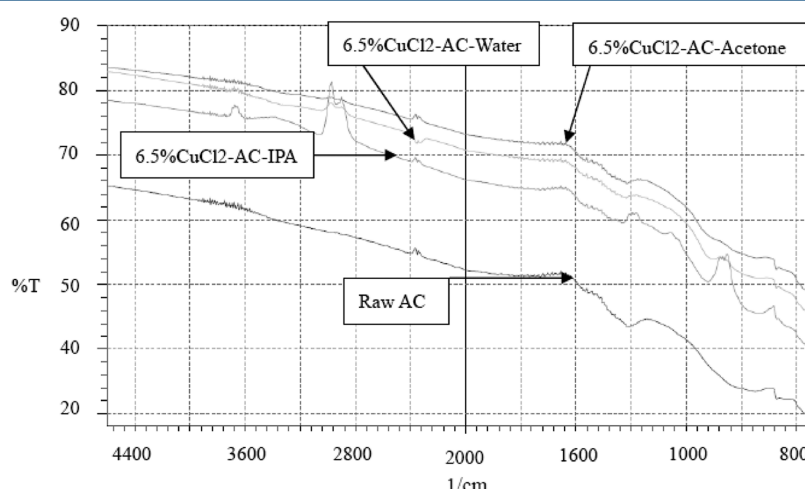


Figure 7. FTIR spectra of the pure sorbents.

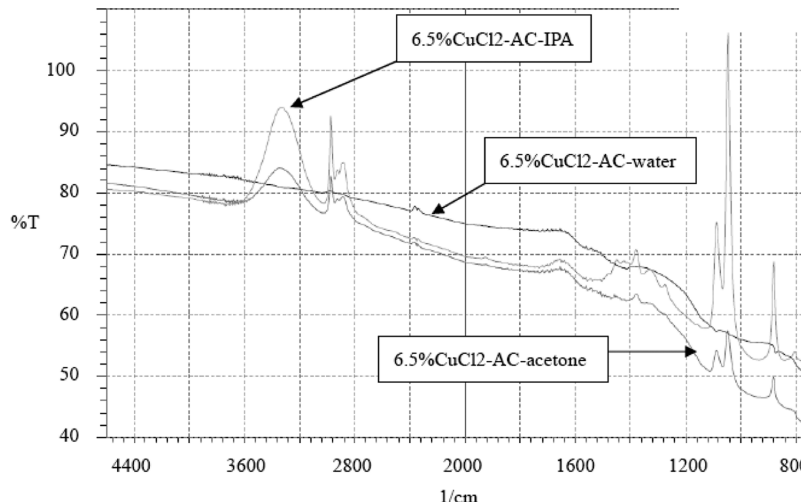


Figure 8. FTIR spectra of the adsorbed sorbents.

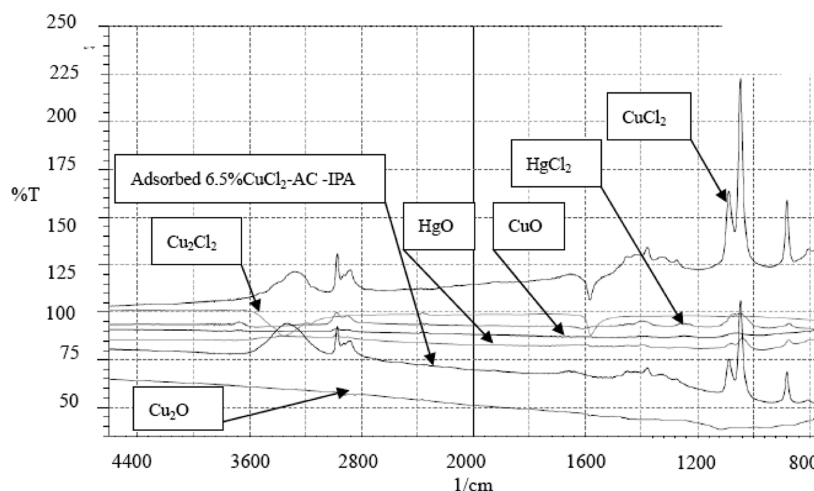


Figure 9. Comparison of FTIR spectra of the adsorbed sorbents with standard salts.

two strong bands at 2830–3060 cm^{-1} and 1020–1117 cm^{-1} can be observed. It is difficult to assign these two bands because there is superposition of a number of broad overlapping bands. Therefore, the bands cannot be described in terms of simple motion of specific functional groups or chemical bonds, but may be bands of a certain state of adsorbed cupric chloride because they have the similar form as peaks at 2976, 2887, 1044, and 879 cm^{-1} , which are of pure cupric chloride, shown in Figure 9.

For AC-IPA and AC-acetone, the experimental procedure strongly increases the appearance of bands at 2945–2050 cm^{-1} , 2910–2950 cm^{-1} , 2800–2910 cm^{-1} and 1200–1483 cm^{-1} , which are due to the reaction between cupric chloride and elemental mercury. The inherent vibration frequency of mercuric chloride³⁴ may increase the intensity of the vibration of these regions, as mentioned above. Comparing the FTIR spectra of the adsorbed sorbents with that of mercuric chloride and mercuric oxide in Figure 10, similar IR images suggest that both mercury chloride and mercuric oxide may also exist on the surface of adsorbed activated carbon. Because no similarity existed between the infrared spectra of mercury oxide and that of adsorbed AC-IPA, it can be confirmed that no mercury oxide was present on the adsorbed AC-IPA.

3.5. Thermogravimetric Analysis. Ten milligrams of adsorbed carbon and raw AC were heated in a small platinum

tube oven under a flow ($35 \text{ mL}\cdot\text{min}^{-1}$) of pure N_2 (one comparison sample under pure oxygen). The heating rate was $5 \text{ }^{\circ}\text{C}\cdot\text{min}^{-1}$ to a temperature of $700 \text{ }^{\circ}\text{C}$. The gases evolved were analyzed by a mass spectrometer, which was coupled to a Pfeiffer Vacuum Thermo-Star TM mass spectrometer equipped with a channeltron detector. The evolved gas was ionized and its components detected according to the mass to charge ($\text{m}\cdot\text{z}^{-1}$) ratio. The system was calibrated with calcium oxalate monohydrate.

Figure 11 depicts derivative weight thermograms of activated carbon before and after cupric chloride modification in IPA solution. TGA curve *a* showed the raw activated carbon using pure nitrogen as both the purge and protective gases, while curves *b* and *c* were TGA analyses of mercury-adsorbed AC under nitrogen and oxygen gas, which were cupric chloride-impregnated in IPA solution. During the pyrolysis process, the weight of three modified AC decreased slightly when the temperature increased in first stage. The received surface modified AC appeared to have its first degradation peaks at approximately $200 \text{ }^{\circ}\text{C}$ (curve *b* and *c*). The total weight loss was approximately 4% in this degradation stage, which may be primarily due to the decomposition of functional groups containing two oxygen atoms, such as carboxylic acids groups.²⁴ An effect of the amount of surface oxygen on the second

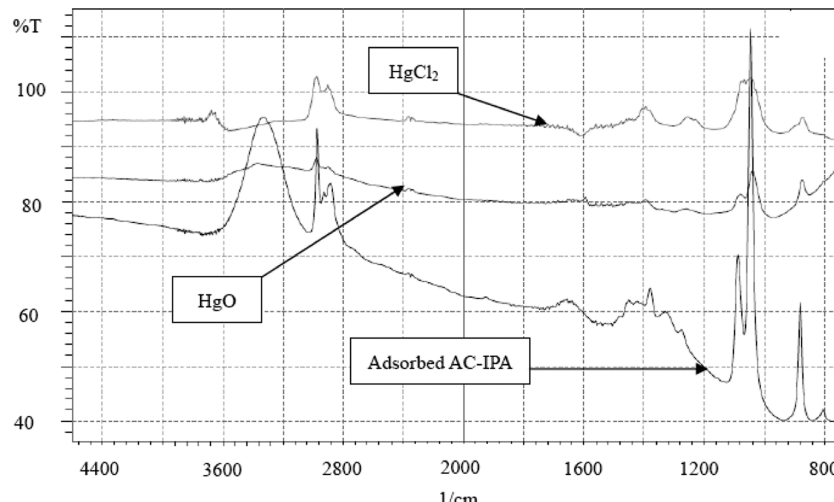


Figure 10. Comparison of FTIR spectra of the adsorbed sorbents with mercuric chloride and mercuric oxide.

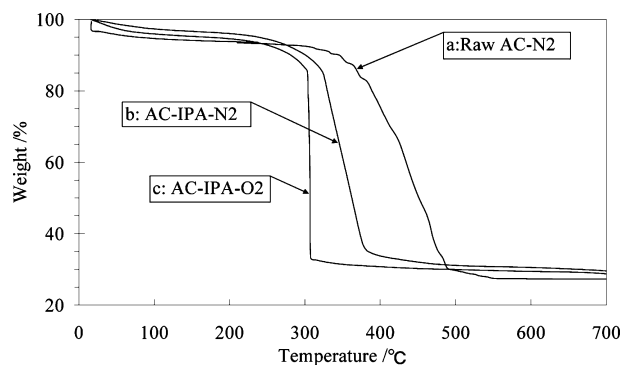


Figure 11. TGA curves of virgin activated carbon and cupric chloride impregnated activated carbons.

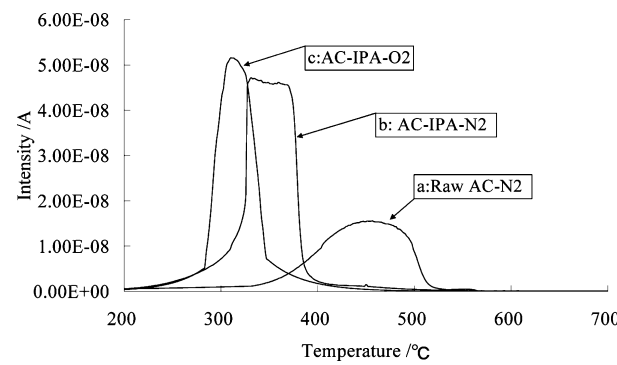


Figure 12. TGA-MS graphs of AC showing the formation of CO₂ as a function of temperature.

degradation peaks can be seen in Figure 11. The amount of surface oxygen groups increased after modification and the pyrolysis temperature of the AC decreased from approximately 400 °C (curve a) to 350 °C (curve b) because more oxygen was involved in the decomposition reaction in the process of heat treatment. The CuCl₂-AC-IPA were heated under pure oxygen gas in the TGA experiment, and the degradation peaks of this situation (curve c) were at 300 °C, indicating a surplus of oxygen in the pyrolysis gas phase.

It has been reported that the modified AC contains many surface organic oxygen groups, which are thermally less stable and more easily form carbon dioxide and carbon monoxide in the process of thermal decomposition.³⁵ It is well accepted that surface groups derived from carboxylic acids such as anhydrides, lactones, and the acids themselves, yield predominantly CO₂ upon decomposition, whereas CO is formed during the decomposition of functional groups containing one oxygen atom.³⁶

Figure 12 shows the intensity of the CO₂ released after pyrolysis of different activated carbons. Curves a and b show before and after cupric chloride modification in IPA solution. Curves b and c show the TGA-MS analysis of mercury-adsorbed AC under nitrogen and oxygen gas, respectively, which were cupric chloride-impregnated in IPA solution. In general, CO₂ is formed at lower temperatures, whereas CO is formed at higher temperatures. From the TGA-MS graph, CO₂ is slowly formed when the pyrolysis temperature is between

200 and 250 °C for the three types of AC. When the temperature is approximately 280 °C, the intensity of the CO₂ releasing of the AC(c) began to rapidly rise, and the temperature of intensity peak was 310 °C. The maximum formation of CO₂ is significantly dependent on the type of activated carbon. The b carbons all show two CO₂ peaks with maxima of 330 and 380 °C, whereas the a carbon has a single maximum at 470 °C. However, two of the CO₂ intensities are lower than c, and the temperature of the intensity peak of AC(a) is approximately 460 °C. After reaching the maximum formation, the releasing intensity of CO₂ dropped fast with the increasing temperature; whereas, AC(a) is from 470 to 510 °C, AC(b) is from 370 to 390 °C, and AC(c) is from 310 to 350 °C.

4. CONCLUSION

A specific weight of cupric chloride impregnated activated carbon has been found to have a significant effect on mercury adsorption. The results from this study indicate the following:

- (1) The specific surface areas and pore volumes of raw activated carbon were measured and the chemical groups of before and after different concentrations of cupric chloride impregnated activated carbon surfaces were estimated by Boehm titration. The results show that cupric chloride impregnated activated carbon, which used isopropyl alcohol as the solution, significantly increased the functional groups with carboxylic, hydroxyl, and lactones and other oxygen containing groups.

- (2) Three types of cupric chloride impregnated modified activated carbon was studied in Hg adsorption. It is demonstrated that the adsorption capacity for Hg^0 in the cupric chloride impregnated activated carbon in IPA is the greatest, and the amount of Hg^{2+} increases in the outflow gas of adsorption with an increasing load of mercury on activated carbon. Moreover, from the mercury chemisorption data, the copper content does not have a direct influence on the mercury uptake, and the distribution status of copper and its corresponding functional groups play an important role in mercury adsorption.
- (3) FTIR analysis detected the surface functional groups on different kinds of modified activated carbon and compared pure sorbents and adsorbed sorbents on the change in surface groups and reaction products. The bands 3200–3640 cm^{-1} and 2300–2500 cm^{-1} were much weaker than those of the original carbons, demonstrating that hydroxyl groups and carboxyl groups have been changed in the process of chemisorptions, and $\text{CuCl}_2\text{-AC-IPA}$ and $\text{CuCl}_2\text{-AC-acetone}$ have pronounced bands similar to pure cupric chloride. From the unique vibration bands, both were seen in the spectrum of pure cuprous chloride and adsorbed activated carbon. It was illustrated that the cuprous chloride may occur on the adsorbed carbon. Moreover, the experimental procedure increases strongly the appearance of bands was caused by the reaction between cupric chloride and elemental mercury, and no mercury oxide was present on adsorbed AC-IPA.
- (4) TGA analyzed the derivative weight thermograms of activated carbon before and after cupric chloride modification in IPA solution. The weight of the modified activated carbon decreased slightly before 200 °C, and drastic weight loss was present at temperatures between 300 and 400 °C because of more oxygen functional groups involved in decomposition reaction in the process of heat treatment. TGA-MS graphs compared to CO_2 -releasing intensity as the temperature increased with raw and modified activated carbon explains how the decomposition temperature and intensity of CO_2 and CO formed was dependent on surface oxygen functional groups.

AUTHOR INFORMATION

Corresponding Author

*Tel.: +86 -0731-88877195. Fax: +86 -0731-88879863.
E-mail: liqingli@hotmail.com.

Notes

The authors declare no competing financial interest.

ACKNOWLEDGMENTS

The support of the National Science Foundation of China under program 20976200 is gratefully acknowledged.

REFERENCES

- (1) U.S. EPA. *A Study of Hazardous Air Pollutant Emissions from Electric Utility Steam Generator Units*, Final Report to Congress, EPA-453/R-98-004a; U.S. Environmental Protection Agency: Washington, DC, 1998.
- (2) Change, R.; Offen, G. R. Mercury emission control technologies: An EPRI synopsis. *Power Eng.* **1995**, *99*, 51.
- (3) Lee, S. S.; Lee, J. Y.; Keener, T. C. Novel sorbents for mercury emissions control from coal-fired power plants. *J. Chin. Inst. Chem. Eng.* **2008**, *39*, 137.
- (4) Presto, A. A.; Granite, E. J.; Karash, A. Further investigation of the impact of sulfur oxides on mercury capture by activated carbon. *Ind. Eng. Chem. Res.* **2007**, *46*, 8273.
- (5) Vitolo, S.; Seggiani, M. Mercury removal from geothermal exhaust gas by sulfur-impregnated and virgin activated carbons. *Geothermics* **2002**, *31*, 431.
- (6) Lee, S. S.; Lee, J. Y.; Khang, S. J.; Keener, T. C. Modeling of mercury oxidation and adsorption by cupric chloride-impregnated carbon sorbents. *Ind. Eng. Chem. Res.* **2009**, *48*, 9049.
- (7) Hu, C. X.; Zhou, J. S.; He, S.; Luo, Z. Y.; Cen, K. F. Effect of chemical activation of an activated carbon using zinc chloride on elemental mercury adsorption. *Fuel Process. Technol.* **2009**, *90*, 812.
- (8) Vidic, R. D.; Siler, D. P. Vapor-phase elemental mercury adsorption by activated carbon impregnated with chloride and chelating agents. *Carbon* **2001**, *39*, 3.
- (9) Lee, S. S. Modeling and Experimental Studies for the Control of Mercury from Coal Combustion Flue Gas Streams Using Cupric Chloride-Impregnated Sorbents, Ph.D. Dissertation, University of Cincinnati, Cincinnati, OH, 2008.
- (10) Lee, S. S.; Lee, J. Y.; Keener, T. C. The effect of methods of preparation on the performance of cupric chloride-impregnated sorbents for the removal of mercury from flue gases. *Fuel* **2009**, *88*, 2053.
- (11) Padak, B.; Brunetti, M.; Lewis, A.; Wilcox, J. Mercury binding on activated carbon. *Environ. Prog.* **2006**, *25*, 319.
- (12) Li, Y. H.; Lee, C. W.; Gullett, B. K. Importance of activated carbon's oxygen surface functional groups on elemental mercury adsorption. *Fuel* **2003**, *82*, 451.
- (13) Tsuji, K.; Shiraishi, I. Combined desulfurization, denitrification and reduction of air toxics using activated coke: 2. Process applications and performance of activated coke. *Fuel* **1997**, *76*, 555.
- (14) Serp, P.; Figueiredo, J. L. *Carbon Materials for Catalysis*; John Wiley & Sons: Hoboken, 2008.
- (15) Buczek, B.; Biniak, S.; Tkowski, A. Oxygen distribution within oxidised active carbon granules. *Fuel* **1999**, *78*, 1443.
- (16) Haynes, W. M.; Lide, D. R.; Baysinger, G.; Berger, L.; Frenkel, M.; Goldberg, R. N. *CRC Handbook of Chemistry and Physics*, 91st ed.; CRC Press: Boca Raton, FL, 2011.
- (17) Nicholls, D. *Complexes and First-Row Transition Elements*; Macmillan Press: London, 1973.
- (18) Standard Test Method for Elemental, Oxidized, Particle-bound and Total Mercury in Flue Gas Generated from Coal-Fired Stationary Sources, ASTM Method D6784-02; ASTM international, 2006.
- (19) Chen, J. M.; Zhang, J. Application of ASAP2020 specific surface area and porosity analyze. *Anal. Instrum. (china)* **2009**, *3*, 61.
- (20) Davis, M. E. Ordered porous materials for emerging applications. *Nature* **2002**, *417*, 813.
- (21) Boehm, H. P. Some aspects of the surface chemistry of carbon blacks and other carbons. *Carbon* **1994**, *32*, 759.
- (22) Ferro-García, M. A.; Utrera-Hidalgo, E.; Rivera-Utrilla, J.; Moreno-Castilla, C.; Joly, J. P. Regeneration of activated carbons exhausted with chlorophenols. *Carbon* **1993**, *31*, 857.
- (23) Scherdel, C.; Reichenauer, G.; Wiener, M. Relationship between pore volumes and surface areas derived from the evaluation of N_2 -sorption data by DR-, BET- and t-plot. *Microporous Mesoporous Mater.* **2010**, *132*, 572.
- (24) Figueiredo, J. L.; Pereira, M. F. The role of surface chemistry in catalysis with carbons. *Catal. Today* **2010**, *150*, 2.
- (25) Boehm, H. P. Surface oxides on carbon and their analysis: A critical assessment. *Carbon* **2002**, *40*, 145.
- (26) Voll, M.; Boehm, H. P. Basische oberflächenoxide auf kohlenstoff-III aktiver wasserstoff und polare adsorptionszentren. *Carbon* **1971**, *9*, 473.
- (27) Strelko, V.; Malik, D. J.; Streat, M. Characterisation of the surface of oxidised carbon adsorbents. *Carbon* **2002**, *40*, 95.
- (28) Szymański, G. S.; Rychlicki, G. Importance of oxygen surface groups in catalytic dehydration and dehydrogenation of butan-2-ol promoted by carbon catalysts. *Carbon* **1991**, *29*, 489.

- (29) Liu, J.; Marcos, A. C.; Wu, F.; Li, M. Effects of chemical functional groups on elemental mercury adsorption on carbonaceous surfaces. *J. Hazard. Mater.* **2011**, *186*, 108.
- (30) Song, X. L.; Liu, H. Y.; Cheng, L.; Qu, Y. X. Surface Modification of coconut-based activated carbon by liquid-phase oxidation and its effects on lead ion adsorption. *Desalination* **2010**, *255*, 78.
- (31) Menéndez, J. A.; Menéndez, E. M.; Iglesias, M. J.; García, A.; Pis, J. J. Modification of the surface chemistry of active carbons by means of microwave-induced treatments. *Carbon* **1999**, *37*, 1115.
- (32) Moreno-Castilla, C.; López-Ramón, M. V.; Carrasco-Mafrín, F. Changes in surface chemistry of activated carbons by wet oxidation. *Carbon* **2000**, *38*, 1995.
- (33) Liu, Z. Q.; Ma, J.; Cui, Y. H.; Zhang, B. P. Effect of ozonation pretreatment on the surface properties and catalytic activity of multi-walled carbon nanotube. *Appl. Catal., B* **2009**, *92*, 301.
- (34) Saito, T.; Hayamizu, K.; Yanagisawa, M.; Yamamoto, O.; Wasada, N.; Someno, K. Spectral database for organic compounds (SDBS). <http://riodb01.ibase.aist.go.jp/sdbs/> (accessed 2004).
- (35) Vinke, P.; van der Eijk, M.; Verbree, M.; Voskamp, A. F.; van Bekkum, H. Modification of the surfaces of a gasactivated carbon and a chemically activated carbon with nitric acid, hypochlorite, and ammonia. *Carbon* **1994**, *32*, 675.
- (36) Tremblay, G.; Vastola, F. G.; Walker, P. L. Thermal desorption analysis of oxygen surface complexes on carbon. *Carbon* **1978**, *16*, 35.